Journal of Photochemistry and Photobiology A: Chemistry 213 (2010) 52–60

Contents lists available at ScienceDirect

Journal of Photochemistry and Photobiology A: Chemistry

journal homepage: www.elsevier.com/locate/jphotochem

Photophysical, electro- and spectroelectro-chemical properties of the nonplanar porphyrin [ZnOEP(Py)$_4^{4+}$,4Cl$^-$] in aqueous media

N. Karakostas[a], D. Schaming[a], S. Sorgues[a], S. Lobstein[b], J.-P. Gisselbrecht[b], A. Giraudeau[b], I. Lampre[a,*], L. Ruhlmann[a,**]

[a] Laboratoire de Chimie Physique, UMR 8000 CNRS/Université Paris-Sud 11, Faculté des Sciences d'Orsay, Bâtiment 349, 91405 Orsay Cedex, France
[b] Laboratoire d'Electrochimie et de Chimie-Physique du Corps Solide, UMR 7177 CNRS/Université de Strasbourg, 4 rue Blaise Pascal, 67000 Strasbourg Cedex, France

ARTICLE INFO

Article history:
Received 22 February 2010
Received in revised form 15 April 2010
Accepted 25 April 2010
Available online 1 June 2010

Keywords:
Water soluble porphyrin
Pyridinium
Electrochemistry
Spectroelectrochemistry
Absorption
Fluorescence

ABSTRACT

The photophysical and electrochemical properties of the tetracationic zinc 2,3,7,8,12,13,17,18-octaethyl-5,10,15,20-tetrakis(*N*-pyridiniumyl) porphyrin chloride (ZnOEP(Py)$_4^{4+}$,4Cl$^-$) were studied in aqueous solutions. The steady state and time-resolved absorption and emission measurements indicate that the porphyrin skeleton adopts a severely nonplanar conformation which minimizes steric crowding between the 12 peripheral substituents. The absorption spectrum of [ZnOEP(Py)$_4^{4+}$,4Cl$^-$] in water exhibits significant red shifts of the visible Q and Soret bands as well as considerable broadening and decrease in intensity of the latter compared to the spectrum recorded for the planar [ZnTMPyP^{4+},4Cl$^-$] porphyrin. The $S_2 \rightarrow S_1$ internal conversion is faster than the experimental resolution (<90 fs) while the S_1 excited state has a lifetime of 170 ps. The electrochemical properties of [ZnOEP(Py)$_4^{4+}$,4Cl$^-$] were investigated in water at pH 6.5 and 3.0 by cyclic and differential pulse voltammetry as well as spectroelectrochemistry. Reductions take place initially at the pyridinium sites with four successive one-electron steps at pH 6.5 or a one-electron step followed by a three-electron process at pH 3.0. Both oxidation and reduction processes undergone by the porphyrin are irreversible.

1. Introduction

Porphyrins and their derivatives constitute a major class of chemical compounds due to their various optical, physicochemical and redox properties. Naturally occurring porphyrins play essential roles in photosynthesis, cellular respiration and biological electron transfer reactions [1]. Consequently, much attention has been devoted to these compounds with respect to their potential biological and medical applications such as DNA cleavage catalysts [2,3] or photosensitizers in photodynamic therapy [4–9]. Interactions between porphyrin derivatives and DNA have also been the subject of several works [10–16]. But, only a few planar *meso*-substituted water soluble porphyrins, such as 5,10,15,20-tetra(*N*-methyl-4-pyridyl)porphyrins (TMPyP^{4+}), have been investigated.

Studies of the crystal structures of protein complexes formed by porphyrinic chromophores and prosthetic groups have revealed skeletal distortions of the porphyrin macrocycle [17–19]. These findings have consequently stimulated efforts devoted to synthesis of nonplanar model porphyrins, for instance by substituting bulky groups at the peripheral positions of the macrocycle and/or changing the central metal [20,21]. Indeed, it has been shown that the conformational distortion of the skeleton minimizes the steric interactions between its substituents. Most of the dodecasubstituted porphyrins which have been synthesized, exhibit nonplanar, highly distorted structures [22]. That was the case for the first reported dodecasubstituted tetracationic metalloporphyrins that were derived from β-octabromo-*meso*-tetra(*N*-methyl-4-pyridiniumyl)porphyrin [23]. Even if the origin of the changes is controversial [24–26], it is known that macrocyclic deformations can profoundly affect the optical, redox, magnetic, radical and excited-state properties of the porphyrins [27–33].

Substituted metalloporphyrins bearing multiple charges should be of particular interest because they would combine solubility in water and possible interactions with various biological targets such as proteins and nucleic acids. While there are numerous studies in non-aqueous media for conformationally perturbed porphyrins, similar studies in water are rather scarce. The dodecasubstituted and tetracationic zinc porphyrin [(Py)ZnOEP(Py)$_4^{4+}$,4PF$_6^-$] with four pyridinium groups bound at the *meso* position through their nitrogen atom and one axially ligated pyridine, was the first representative of a new class of nonplanar metalloporphyrins bearing four positive charges at a distance shorter than 5 Å from the metal

* Co-corresponding author. Tel.: +33 1 69 15 45 11; fax: +33 1 69 15 61 88.
** Corresponding author. Tel.: +33 1 69 15 44 38; fax: +33 1 69 15 61 88.
E-mail addresses: isabelle.lampre@u-psud.fr (I. Lampre), laurent.ruhlmann@u-psud.fr (L. Ruhlmann).

1010-6030/$ – see front matter © 2010 Elsevier B.V. All rights reserved.
doi:10.1016/j.jphotochem.2010.04.019

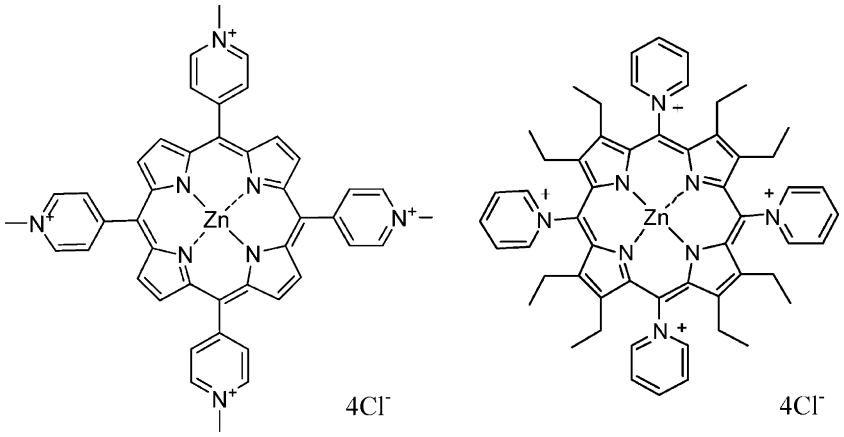

Fig. 1. Simplified structures of the [ZnTMPyP^{4+},4Cl$^-$] (left) and [ZnOEP(Py)$_4{}^{4+}$,4Cl$^-$] (right) porphyrins.

centre [34]. The structure has been resolved in the solid state by crystallography and corresponds to a saddle conformation of the cationic macrocycle with the pyrrole rings (and their alkyl substituents) displaced up and down alternately [34]. By passing this porphyrin through a Cl$^-$ exchange resin column, the counterion is exchanged, the axial pyridine is removed and the water soluble derivative, [ZnOEP(Py)$_4{}^{4+}$,4Cl$^-$] is obtained (Fig. 1) [35].

The present study deals with the photophysical and redox properties of this distorted porphyrin and their relations with the conformation of the macrocycle. In this context, the behavior of [ZnOEP(Py)$_4{}^{4+}$,4Cl$^-$] is compared to that of the planar tetracationic porphyrin [ZnTMPyP^{4+},4Cl$^-$].

2. Experimental

2.1. Materials

ZnOEP (Zn-2,3,7,8,12,13,17,18-octaethyl porphyrin), [ZnTMPyP^{4+},4Cl$^-$] (zinc 5,10,15,20-tetrakis(*N*-methyl-4-pyridyl)porphyrin chloride) and pyridine compounds were of reagent grade quality, purchased from Sigma Aldrich and used without further purification.

The zinc 2,3,7,8,12,13,17,18-octaethyl-5,10,15,20-tetrakis(*N*-pyridiniumyl)porphyrin chloride, [ZnOEP(Py)$_4{}^{4+}$,4Cl$^-$], was synthesized following previous reports [35].

H_2SO_4 solutions, solid Na_2SO_4 and NaOH were commercial products from Prolabo.

Pure water was obtained by passing through a Milli-RO_4 unit and subsequently through a Millipore Q water purification set.

2.2. Photophysical measurements

All photophysical measurements were carried out in water at natural pH at room temperature ($22 \pm 2\,^\circ$C).

Steady-state optical absorption spectra were recorded with a PerkinElmer Lambda 9 spectrophotometer. Steady-state luminescence emission spectra were obtained using a Spex fluorolog 1681 spectrofluorimeter equipped with a Hamamatsu R928 photomultiplier which was cooled to the temperature of $-20\,^\circ$C. The fluorescence spectra were corrected for the detector spectral sensitivity.

Time-resolved fluorescence measurements were carried out using a time-correlated single photon counting set-up. The source was a Ti:sapphire laser (MIRA 900F) pumped by a Nd:YVO_4 laser (VERDI). The repetition rate was reduced to 3.8 MHz and the second harmonic (420 nm, vertically polarized) was generated in a BBO crystal and used to excite the samples. The emission was selected via a polarizer, set at the magic angle (54.7°) with respect to the excitation electric vector. A monochromator was used for wavelength selection and the signals were collected by an optical spectrometric multichannel analyzer.

Laser flash photolysis was performed using third harmonic pulses (355 nm, 3 ns FWHM 10 mJ/pulse) from a Nd:YAG laser (BMI). Detection of the transient species was carried out by an optical absorption set-up, consisting of a pulsed Xe arc lamp, monochromator and photomultiplier. Samples were argon-bubbled aqueous solutions contained in 1 cm path cell.

Femtosecond transient absorption pump–probe experiments were performed with a Ti:sapphire amplified laser system (Spectra Physics) delivering 100 fs pulses at 790 nm, with an energy of 1 mJ at a repetition rate of 1 kHz. The laser beam was splitted into two parts. The main part is used to produce the pump beam at 395 nm by frequency doubling in a BBO crystal. The pump pulses were then attenuated to 10 μJ and focused to a 0.5 mm beam on the sample. After travelling along an optical delay line, the small fraction of the Ti:sapphire output was used for white light continuum generation in a 3 mm sapphire crystal. This white light beam was divided before the cell and used in the one hand as the probe beam and in the other hand as a reference beam (unaffected by the pump). The pump and probe beams overlapped in a fused silica sample cell with 1 mm path, and their polarizations were set at the magic angle. The detection system consisted of an imaging polychromator and a CCD camera (1340 × 400 Princeton Instruments). Measurements were performed in aerated solutions. The spectra were corrected for the group velocity dispersion (GVD).

2.3. Electrochemical and spectroelectrochemical measurements

All electrochemical measurements were carried out under argon at 20 °C on a glassy carbon disk electrode (d = 3 mm). Voltammetric data were obtained with a standard three-electrode system using a PARSTAT 2273 potentiostat. A platinum wire was used as an auxiliary electrode. The reference electrode was a saturated calomel electrode (SCE). It was electrically connected to the solution by a junction bridge filled with water containing the supporting electrolyte. The electrolyte was made up from 0.5 M Na_2SO_4 aqueous solution, and its pH was precisely adjusted to 3.0 by addition of 0.5 M H_2SO_4 aqueous solution and to pH 6.5 by addition of NaOH. The solutions were deaerated thoroughly for at least 30 min by bubbling argon (Ar–U from Air Liquide) and kept under argon atmosphere during the whole experiment.

For the spectroelectrochemical studies, a standard three-electrode system was used with a Bruker EI 30 M potentiostat and high-impedance millivoltmeter (Minisis 6000, Tacussel), in H_2O

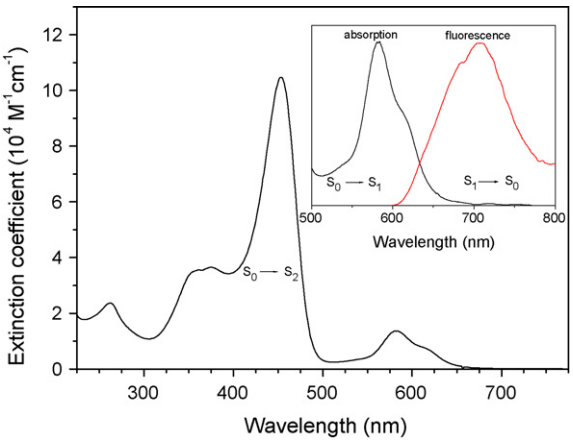

Fig. 2. Ground state absorption of [ZnOEP(Py)$_4^{4+}$,4Cl$^-$] in water; inset: Q bands absorption and steady-state fluorescence spectra of [ZnOEP(Py)$_4^{4+}$,4Cl$^-$] in water (1 cm path length cell, excitation wavelength: 570 nm).

and using an OTTLE (optically transparent thin layer electrode). The working electrode was a Pt mini grid (100 mesh). The spectra were recorded on a Hewlett Packard 8452 A diode array spectrophotometer. The thin layer spectroelectrochemical cell has been previously described by Bernard et al. [36].

3. Results and discussion

3.1. Photophysical properties

The photophysical data of [ZnOEP(Py)$_4^{4+}$,4Cl$^-$] and some reference porphyrins are gathered in Table 1.

The ground state absorption spectrum of [ZnOEP(Py)$_4^{4+}$,4Cl$^-$] in water, illustrated in Fig. 2, resembles that of the parent porphyrin [(Py)ZnOEP(Py)$_4^{4+}$,4PF$_6^-$] in acetonitrile [34]. The Soret and Q bands are red-shifted and characterized by a reduced peak intensity and a significant broadening in comparison to the spectrum of the precursor ZnOEP [37] (Table 1). Such a behavior is partially due to the presence of the electron-withdrawing character of the pyridinium substituents [38] but mainly attributed to distorted conformations of the macrocycle ring. Indeed, the saddle-shaped porphyrin ZnOETPP [39] presents similar positions of the bands (Table 1), red-shifted compared to the planar *meso*-substituted porphyrins ZnTPP [37,40] and ZnTMPyP^{4+} [38,41]. Numerous papers give evidence of red shifts in the optical absorption bands of highly substituted nonplanar porphyrins [18,19,25,26,42–44]. The red-shifts are explained by larger destabilization of the highest occupied molecular orbitals (HOMOs) relative to the lowest unoccupied molecular orbitals (LUMOs) resulting in smaller HOMO to LUMO gaps [19–21,32,39].

The fluorescence emission spectrum of ZnOEP(Py)$_4^{4+}$ in water (inset in Fig. 2) presents a broad almost featureless band centred near 700 nm. Due to the poor resolution of the Q bands, the absorption/emission "Stokes" shift is estimated between the Q(0,0) absorption band (shoulder at 620 nm in the absorption spectrum) and the fluorescence maximum (710 nm) and found to be around 2040 cm^{-1}. This value is of the same order of magnitude as the shift reported for the saddle-shaped porphyrin, ZnOETPP, in organic solvents (1660 cm^{-1}) [43] but, three times as high as that determined for the planar cationic porphyrin ZnTMPyP^{4+} in water (640 cm^{-1}) [41]. It has been suggested that such shift and emission profile reflect photoinduced changes in macrocycle conformation [43,45]. Using ZnTMPyP^{4+} as a reference (Φ_{fl} = 0.025 in water) [38] and 570 nm as the excitation wavelength, the fluorescence quantum yield (Φ_{fl}) of ZnOEP(Py)$_4^{4+}$ at room temperature was estimated to be 0.0025. This quantum yield is low, one tenth of the value obtained for the planar ZnTMPyP^{4+} in water but it is of the same order of magnitude as those reported for conformationally perturbed porphyrins [29,43] (Table 1). From time-resolved fluorescence measurements by the single photon counting technique, the S_1 excited-state lifetime of ZnOEP(Py)$_4^{4+}$ is found to be $\tau_S = 170 \pm 20$ ps. This value is identical to the lifetime determined for ZnOETPP in toluene but roughly ten times shorter than the lifetimes of the planar analogues ZnTMPyP^{4+} [41], ZnTPP [37,40,43,46] or ZnOEP [37] (Table 1). The radiative (k_r) and non-radiative (k_{nr}) rate constants are evaluated from τ_S and Φ_{fl} using the following equations:

$$\tau_S = \frac{1}{k_r + k_{nr}} \quad (1)$$

Table 1
Photophysical parameters of [ZnOEP(Py)$_4^{4+}$,4Cl$^-$] measured in water and some reference porphyrins.

Porphyrin	Solvent	UV–vis absorption		Fluorescence					Triplet
		λ_{max}/nm (ε/10^3 dm^3 mol^{-1} cm^{-1})		λ_{max}/nm	Φ_{fl}	τ_S/ns	k_r/10^7 s^{-1}	k_{nr}/10^8 s^{-1}	τ_T/μs
		Soret	Q(1,0), Q(0,0)						
ZnOEP(Py)$_4^{4+}$	Water[a]	453 (105)	584 (13.7), 620	710	0.0025	0.170	1.47	58.7	110
ZnTMPyP^{4+}	Water[b]	436 (180)	562 (16.0), 602 (5.3)	626, 666	0.025	1.3	1.90	7.50	2000
ZnOETPP	CH_2Cl_2[c]	454 (202)	586 (13.1), 637 (5.5)	N.a.	N.a.	N.a.	N.a	N.a.	N.a.
	Toluene[d]	N.a.	N.a., 655	735	0.003	0.15	2.0	66.5	N.a.
ZnOEP	Toluene[e]	404 (373)	N.a., 578 (20.1)	574	0.068	2.00	3.39	4.66	N.a.
ZnTPP	Toluene	423 (442)[e]	N.a, 588 (24.5)[e]	597[e]	0.03[d]	1.9[d]	1.58	5.11	1200[h]
	Toluene[f]	422 (255)	548 (9.72), 588 (1.90)	596, 647	0.033	1.98	1.69	4.88	24
	Ethanol[e]	422 (658)	N.a., 596 (21.7)	603	0.0267	1.96	1.36	4.97	N.a.
	Ethanol[g]	N.a.	N.a.	N.a.	0.0267	1.88	1.42	5.14	N.a.

Φ_{fl}: quantum yield of fluorescence, τ_S: lifetime of the singlet state (fluorescence lifetime), τ_T: lifetime of the triplet state, k_r and k_{nr} radiative and non-radiative rate constants for the relaxation of the singlet state, N.a. data not available.

[a] This work.
[b] From [41], [38] and [48].
[c] From [39].
[d] From [43].
[e] From [37].
[f] From [40].
[g] From [46].
[h] In organic solvents from [47].

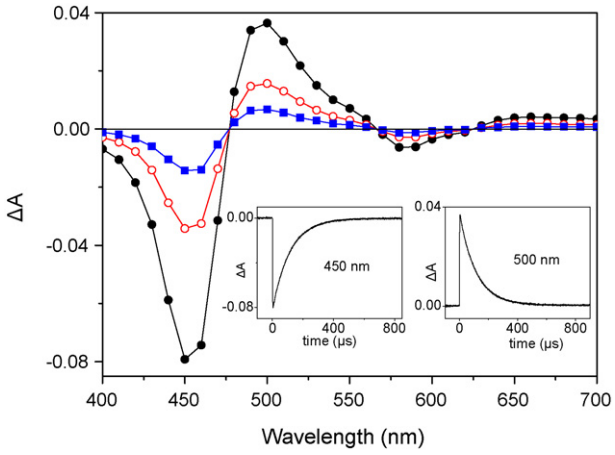

Fig. 3. Transient absorption spectra of a 3.8×10^{-6} M deaerated aqueous solution of [ZnOEP(Py)$_4^{4+}$,4Cl$^-$] recorded upon nanosecond laser photolysis at (●) 5 μs, (○) 100 μs and (■) 200 μs after the 355 nm pulse; insets: time profiles at 450 and 500 nm.

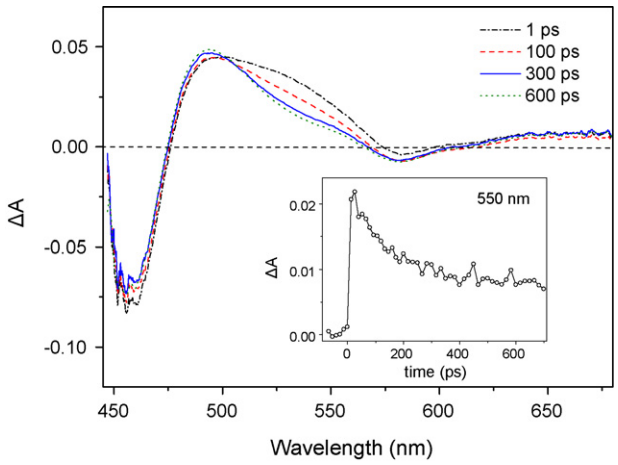

Fig. 4. Transient absorption spectra of a 1.4×10^{-4} M [ZnOEP(Py)$_4^{4+}$,4Cl$^-$] aqueous solution at pH 7 (0.02 mol dm^{-3} phosphate buffer) measured by femtosecond pump-probe technique at different time delays after 395 nm pulse excitation. Inset: time profile at 550 nm.

$$\Phi_{\mathrm{fl}} = \frac{k_r}{k_r + k_{nr}} \tag{2}$$

$$k_r = \frac{\Phi_{\mathrm{fl}}}{\tau_S} \tag{3}$$

$$k_{nr} = \frac{1 - \Phi_{\mathrm{fl}}}{\tau_S} \tag{4}$$

The rate constants found for ZnOEP(Py)$_4^{4+}$ are close to those determined for the saddle-shaped ZnOETPP [43]. The values in Table 1 reveal that the radiative rate constant, k_r, is influenced by the presence of *meso*-substituents as there is a factor two between the radiative rate constants of ZnOEP and ZnTPP in toluene, but k_r is hardly affected by the deformations of the macrocycle. In contrast, the non-radiative rate, k_{nr}, increases by approximately a factor twelve due to distortions of the macrocycle. That indicates an increase in the internal conversion and intersystem crossing rates due to structural deformations.

Fig. 3 depicts the transient absorption spectra obtained by nanosecond pulse photolysis at 355 nm with an Ar saturated aqueous solution of [ZnOEP(Py)$_4^{4+}$,4Cl$^-$]. The spectra show the bleaching of the ground state Soret and Q bands (around 450 nm and 580 nm, respectively) and two positive excited-state absorption domains, one intense with a maximum at 500 nm and a weaker broad absorption area extending beyond 640 nm. The time profiles exhibit clear first order kinetics with a lifetime of 110 μs throughout the spectrum (insets in Fig. 3). The presence of oxygen accelerates the relaxation processes resulting in a time constant of 6.4 μs. So, the observed transient signals are attributed to the triplet state T_1 of ZnOEP(Py)$_4^{4+}$. The found triplet lifetime is shorter than the values in the microsecond range reported for the planar analogues [38,47] despite some discrepancies in the literature [40,48]. The presence of the triplet state is recorded immediately after the laser pulse and in the nanosecond time scale it was not possible to observe any excited-state precursor of T_1. The employment of femtosecond photolysis provided the means to overcome this obstacle.

Fig. 4 shows the transient absorption spectra obtained after excitation by femtosecond pulses at 395 nm. Very similar spectra and time profiles were obtained when the experiments were repeated in pH 3.0 and pH 7.0 buffered solutions. The spectrum at 1 ps exhibits the bleaching of the Soret and Q bands as well as a strong broad absorption domain around 525 nm along with a weak absorption feature over 650 nm. For a few hundreds of picoseconds, the differential absorbencies, ΔA, around 530 nm drop, while ΔA at other wavelengths remain almost constant. At 600 ps after femtosecond excitation, the recorded transient spectrum resembles that obtained by nanosecond photolysis (Fig. 3). The transient signals around 530 nm (Fig. 4 inset) follow exponential decays with a time constant of 150 ps to a plateau. This time constant is in good agreement with the S_1 lifetime determined by fluorescence measurements. Consequently, we consider that the observed picosecond spectra are due to the S_1 state and to the $S_1 \rightarrow T_1$ intersystem crossing. This transformation is hardly accompanied by recovery of the ground state. So, the long lasting triplet state of the porphyrin (Fig. 3) is formed within a few hundred ps with a high quantum yield.

It is to be noted that the picosecond absorption spectra were recorded upon excitation on the blue side of the Soret band. When a porphyrin is irradiated in the region of the Soret band it is excited to the S_2 state. There are few reports of direct observation of the S_2 state, typically by means of up-conversion fluorescence [31,49–54]. In most porphyrins rapid relaxation ($S_2 \rightarrow S_1$) takes place and the transient absorption and emission spectra are dominated by S_1. The lifetimes recorded for S_2 usually range between 150 fs and 2.5 ps depending on the nature of the porphyrin (substituents, metal) and the environment (solvent or matrix [55]). Such lifetimes correspond to very fast processes that occur in the same time range as the dynamic phenomena of the macrocycle. In some cases, the presence of the S_2 state has been identified with femtosecond absorption experiments [50,53]. Usually, it appears as stimulated emission ($S_2 \rightarrow S_0$) which modifies the shape of the bleaching band. In the case of ZnOEP(Py)$_4^{4+}$ stimulated emission near the Soret band was not observed. Additionally, there was no change in absorbance during the first few picoseconds after the pulse. Hence, we conclude that the S_2 state lifetime is shorter than the instrumental time resolution (less than 90 fs).

In the case of the nanosecond experiment, due to the laser used, excitation was formed at 355 nm. Such excitation generates vibrationally excited S_2 and high-lying singlet (N band) states. As internal conversion and vibrational relaxation in the high-lying singlet and triplet states are known to be in the fs time scale, for both nanosecond and picosecond experiments, the observed long lasting state corresponds to the same lowest triplet state T_1. However, by changing the excitation wavelength, the T_1 formation yield may vary.

In summary, ZnOEP(Py)$_4^{4+}$ exhibits photophysical properties typical of deformed porphyrins. The lowest singlet excited state of a porphyrin has a lifetime determined by its typical decay path-

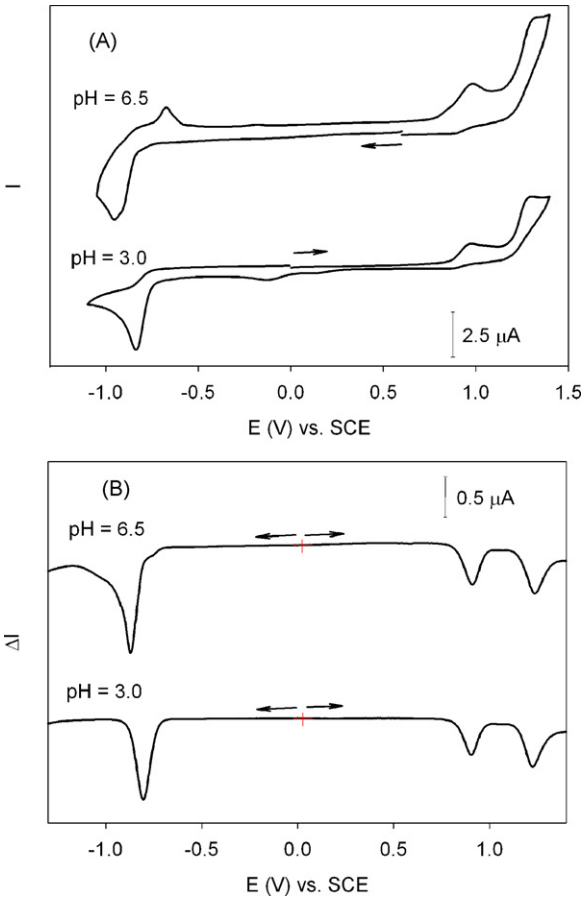

Fig. 5. (A) Cyclic voltammograms (scan rate 100 mV s^{-1}) and (B) differential pulse voltammograms (scan rate 20 mV s^{-1}) of 1×10^{-3} M [ZnTMPyP^{4+},4Cl$^-$] in a 0.5 M $Na_2SO_4 + H_2SO_4$ aqueous solution adjusted at pH 6.5 and 3.0.

ways, i.e. intersystem crossing (to triplet state), internal conversion and fluorescence (to ground state). Distortions of the macrocycle, apart from red shifts of the Soret and Q bands, result in increased intersystem crossing and internal conversion rates and, hence, in reduced fluorescence quantum yields. Moreover, the excited-state lifetimes are shortened.

3.2. Cyclic and differential pulse voltammetry

The electrochemistry of metalloporphyrins incorporating non-electroactive metals has long established that the porphyrin π-system can undergo two reversible one-electron oxidations and reductions to yield π-cation radicals and dications and π-anion radicals and dianions, respectively [56,57]. Additional electron transfers can be observed when the ring bears electroactive groups [58–65] or when protonation reactions occur [66]. Several electrochemical studies of TMPyP^{4+} derivatives have been performed by cyclic voltammetry in aqueous [67–77] or in nonaqueous media [78–82].

Cyclic and differential pulse voltammetry curves of [ZnTMPyP^{4+},4Cl$^-$] and [ZnOEP(Py)$_4{}^{4+}$,4Cl$^-$] in aqueous solutions at pH 3.0 and 6.5 are depicted in Figs. 5 and 6, respectively and the redox data are gathered in Table 2.

The electrochemical behavior in oxidation and reduction of [ZnTMPyP^{4+},4Cl$^-$] in aqueous solution is similar at pH 6.5 and 3.0 (Fig. 5). In the oxidation domain, two successive irreversible peaks are observed at +0.91 and +1.24 V vs. SCE at pH 6.5 (at 0.91 and 1.22 V, respectively, at pH 3.0). They were attributed to the porphyrin ring oxidation leading to a π-cation radical and dication, which can react further with water as already reported [83]. In reduction only one irreversible peak is seen at −0.87 V at pH 6.5 (−0.81 V at pH 3.0). The latter process is assigned to the simultaneous reduction of the four methylpyridinium groups as well as the two-electron reduction of the π-ring system. Indeed, experiments in aqueous solutions have shown that the TMPyP^{4+} derivatives are initially reduced at the π-ring system to give π-anion radicals [69,71,73,76,77] which are usually unstable in water and ultimately converted to phlorins or chlorins [73,76]. Similar results were reported by Neumann-Spallart and Kalyanasundaran for [ZnTMPyP^{4+},4Cl$^-$] in aqueous 0.2 M Na_2SO_4 solution [41,69]. Zhou et al. also observed a single irreversible reduction step for [ZnTMPyP^{4+},4Cl$^-$] in ammoniac buffer solution at pH 8.8 [77]. However, those results differ from other electrochemical studies [84,85], in which two reduction waves were observed.

In contrast to [ZnTMPyP^{4+},4Cl$^-$], the electrochemical behavior of [ZnOEP(Py)$_4{}^{4+}$,4Cl$^-$] differs as a function of pH (Fig. 6). At pH 6.5, the cyclic voltammograms present four irreversible waves, three in reduction (peaks a, b, and c, d) and one in oxidation (peak e). The latter signal at E_{pa} = +1.10 V corresponds to the oxidation of the porphyrin macrocycle and the formation of the porphyrin π-radical cation. The irreversible step at +0.46 V (peak h) on the reverse scan (Fig. 6A) may be associated to reduction of decomposition products.

The reduction processes are not well defined. Nevertheless, the use of differential pulse voltammetry (DPV) mode (Fig. 6A′) reveals the existence of four reduction peaks at −0.58, −0.67, −0.80 and −0.85 V vs. SCE, attributed to the successive reductions of the four pyridinium substituents. Similar behavior was observed in CH_3CN [35].

Each reduction steps become progressively more cathodic as the positive charge of each pyridinium substituent is neutralized and the complex is less positively charged. If the substituents were independent electroactive sites only a single (four-electrons) reduction step would be observed [59,62]. The multisteps reduction indicates the existence of interactions between the four pyridinium groups. It is worth noticing that the reduction of the porphyrin ring occurs beyond the electrolyte discharge and is therefore not observed.

The reduction steps of the four pyridinium (peaks a, b, c and d) as well as for the oxidation step of the porphyrin (peak e) are irreversible indicating that the pyridyl radicals generated after reduction and the porphyrin π-radical cation are not stable and react further.

When the potential scan is reversed after the fourth reduction process, two additional oxidation processes appear on the anodic sweep at +0.81 and +0.95 V vs. SCE (peaks g and f in Fig. 6A). These two peaks are not observed upon direct anodic scan where only the irreversible charge transfer corresponding to the oxidation of the porphyrin ring at +1.10 V (peak e) is recorded. Such oxidation signals obtained from reverse scans may be attributed to the oxidation of dimeric or oligomeric species resulting from a coupling at the 4-position of the pyridyl radicals generated by reduction of the pyridinium substituents (Scheme 1) as already reported [86–89].

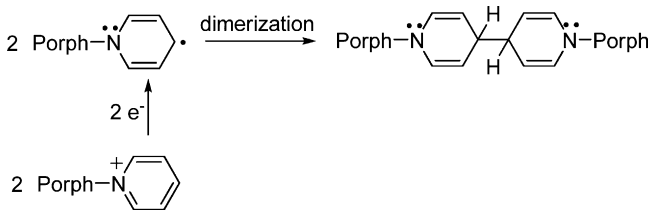

Scheme 1. Electrochemical dimerization mechanism upon reduction of pyridinium cations.

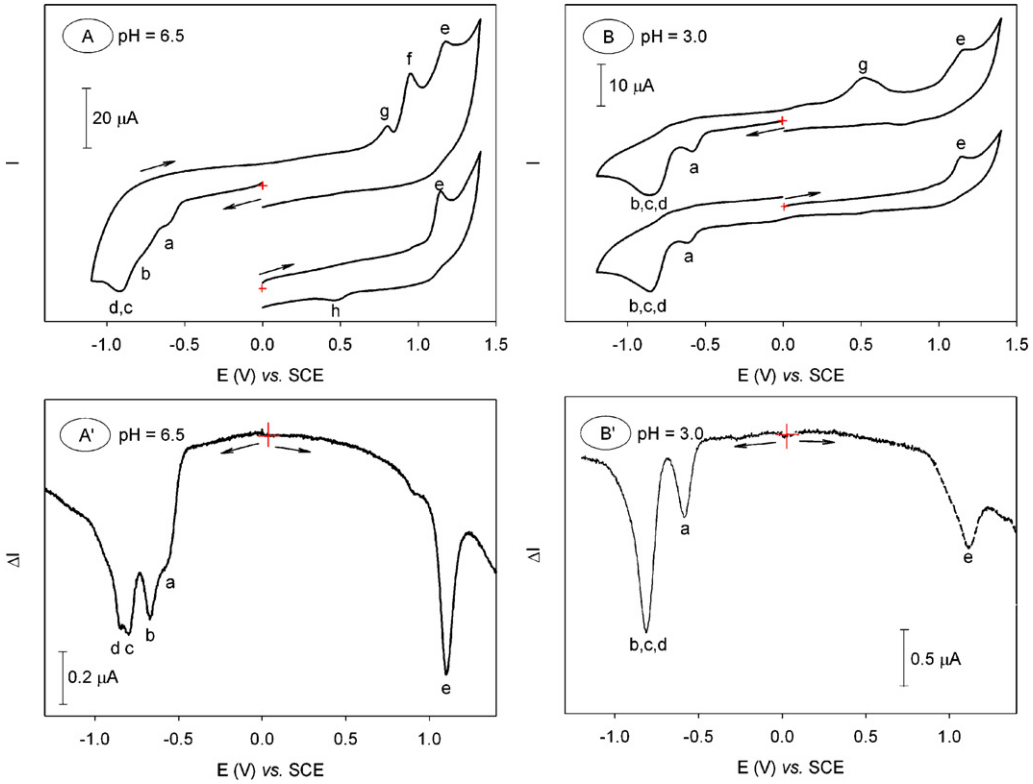

Fig. 6. (A, B) Cyclic voltammograms (scan rate 100 mV s^{-1}) and (A′, B′) Differential pulse voltammograms (scan rate 20 mV s^{-1}) of 5×10^{-4} M [ZnOEP$(Py)_4{}^{4+}$,$4Cl^-$] in a 0.5 M $Na_2SO_4 + H_2SO_4$ aqueous solution adjusted at pH 6.5 and 3.0.

Table 2
Electrochemical data for [ZnOEP$(Py)_4{}^{4+}$,$4Cl^-$] and [ZnTMPPyP^{4+},$4Cl^-$] in aqueous media.

pH	Porphyrins	Oxidation porphyrin ring		Reduction pyridinium
3.0	[ZnTMPyP^{4+},$4Cl^-$]	0.91, 1.24		−0.81
	[ZnOEP$(Py)_4{}^{4+}$,$4Cl^-$]	1.12 (peak e)	0.52[a] (peak g)	−0.59, −0.82
6.5	[ZnTMPyP^{4+},$4Cl^-$]	0.91, 1.22		−0.87
	[ZnOEP$(Py)_4{}^{4+}$,$4Cl^-$]	1.10 (peak e)	0.81[a] (peak g) 0.95[a] (peak f) 0.47 (peak h)	−0.58, −0.67, −0.80, −0.85

All potentials in V vs. SCE are obtained from cyclic voltammetry in H_2O containing 0.5 M $Na_2SO_4 + H_2SO_4$ adjusted to pH 6.5 and 3.0. $\nu = 0.1$ V s^{-1}. WE: glassy carbon. All peaks are irreversible.

[a] Obtained on reversal of the potential sweep after reduction of the pyridinium substituents.

At pH 3.0, only two irreversible reduction steps are present at −0.59 and −0.82 V, respectively (Fig. 6B). The first reduction step occurs at almost the same potential as at pH 6.5 but the following three processes are now unresolved (processes dependent on pH). Differential pulse voltammogram (Fig. 6B′) showed also two reduction steps corresponding to the exchange of one and three electrons, respectively.

This evolution may indicate a loss of conjugation between the pyridinium substituents after the first reduction. That could be the consequence of a protonation on the nitrogen atom of the reduced pyridinium, facilitated by the high acidity (pH 3.0) of the solvent. If the enamine of Scheme 2 is basic enough then the fast protonation could take place before the uptake of the further electrons by ZnOEP$(Py)_4{}^{4+}$.

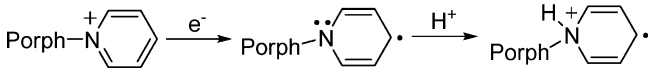

Scheme 2. Electrochemical reduction followed by protonation of the pyridinium cations.

After the reduction processes at pH 3.0, on the reverse scan, a single irreversible signal appears at 0.52 V vs. SCE (peak g) before the irreversible oxidation process of the porphyrin ring at 1.12 V (peak e). As previously suggested, this additional peak is attributed to the formation of dimers (Scheme 1).

Comparing the electrochemical behavior of the two studied porphyrins, it is found that the deformed porphyrin, [ZnOEP$(Py)_4{}^{4+}$,$4Cl^-$], is harder to oxidize than the planar analogue [ZnTMPyP^{4+},$4Cl^-$] (Table 2). This result differs from those of previous studies which report that neutral nonplanar porphyrins were easier to oxidize and harder to reduce than planar porphyrins [17,27]. This apparent contradiction might be explained by the localization of the four positive charges which are closer to the macrocycle in the case of ZnOEP$(Py)_4{}^{4+}$ compared to ZnTMPyP^{4+}.

3.3. Spectroelectrochemistry

Spectroelectrochemical studies were carried out on the reduction of [ZnOEP$(Py)_4{}^{4+}$,$4Cl^-$] under the same experimental conditions as the electrochemical measurements (i.e. in 0.5 M Na_2SO_4 in H_2O and pH 6.5 or pH 3.0). The optical absorption spectra

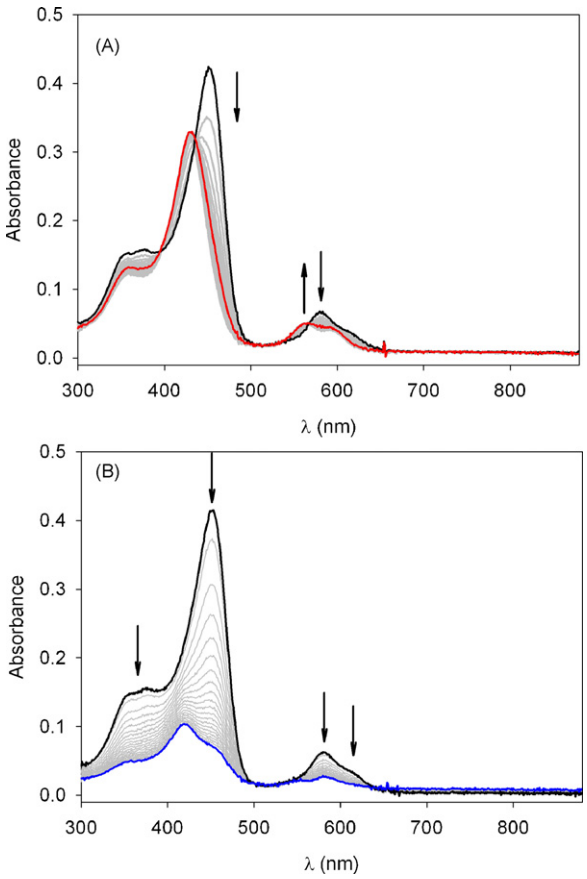

Fig. 7. Evolution of the UV–vis absorption spectrum of an aqueous solution of $[ZnOEP(Py)_4{}^{4+},4Cl^-]$ at pH 6.5 recorded during reduction (A) at −0.70 V and (B) at −1.00 V vs. SCE.

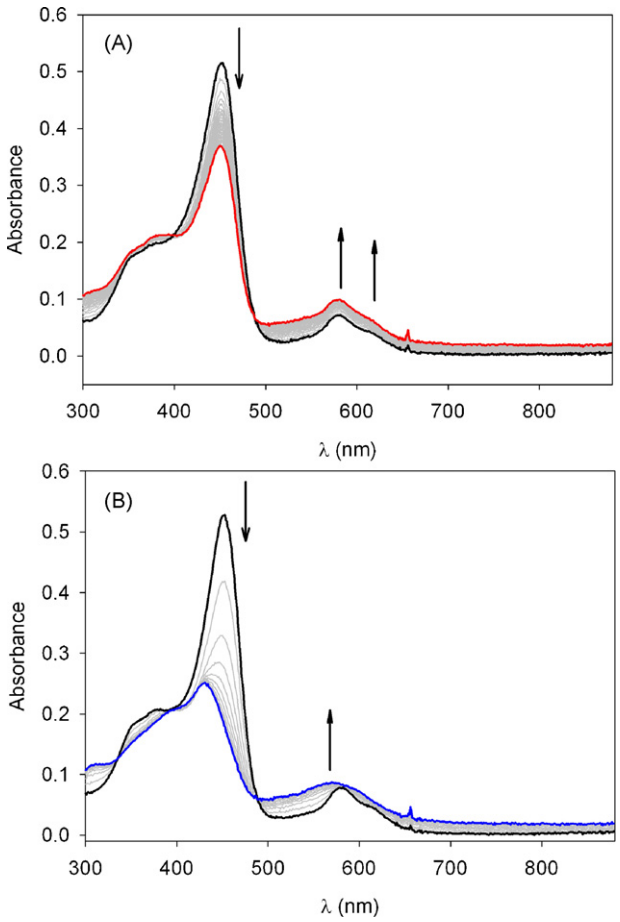

Fig. 8. Evolution of the UV–vis absorption spectrum of an aqueous solution of $[ZnOEP(Py)_4{}^{4+},4Cl^-]$ at pH 3.0 recorded during reduction (A) at −0.65 V and (B) at −1.00 V vs. SCE.

of the systems studied can be used as an additional support to the assignments of the observed redox steps.

For $[ZnOEP(Py)_4{}^{4+},4Cl^-]$ aqueous solution at pH 6.5, the spectral changes recorded during electrolysis at the second reduction wave at −0.70 V vs. SCE, are illustrated in Fig. 7A. From our voltammetric measurements, this potential has been assigned to the second reduction step of the four pyridinium cations in the metalloporphyrin–pyridinium systems. The reduction product exhibits a typical porphyrin spectrum profile with a blue shift of the Soret and Q bands by 20 and 13 nm, respectively, when compared with the parent compound. This result indicates that the electrons are not transferred to the porphyrin macrocycle but to the pyridinium cations and confirms our primary assignment. The blue shift is attributed to the electron-withdrawing effect of only two positively charged pyridiniums in comparison with the starting porphyrin bearing four positively charged substituents. The initial spectrum was not recovered after reverse electrolysis at 0 V in agreement with the cyclic voltammetry experiments where irreversibility of the system was observed. The spectra recorded during reduction at −1.00 V (Fig. 7B) are mainly characterized by a decrease in the intensity of the Soret and Q bands, accompanied with a shift to shorter wavelengths by 21 nm for the Soret band. The formation of a final neutral complex which is not soluble in water and precipitates can account for the flattening of the whole UV–vis spectra.

It is to be noted that, during both electrolysis, no new spectral feature in the domain above 620 nm is observed, which could indicate the presence of a reduction product of the porphyrin ring (dianion, phlorin or chlorin).

Fig. 8A depicts the spectral evolution of $[ZnOEP(Py)_4{}^{4+},4Cl^-]$ aqueous solution at pH 3.0 upon the first one-electron reduction step of the metalloporphyrin–pyridinium system at −0.65 V vs. SCE. During the electrolysis, the intensity of the Soret band decreases slightly and no new peak appears, indicating that the porphyrin ring is not reduced. Moreover, no significant shift is observed. This behavior can be explained by the reduction of a pyridinium cation followed by a protonation of the formed pyridyl radical, since, in this case, there is no change in the overall charge carried by the ring (Scheme 2). As expected from voltammetric data, the spectrum of the initial compound is not recovered after reverse electrolysis at 0 V. The pyridyl radicals are not stable on the cyclic voltammetry time scale, as indicated by the irreversibility of the reduction (Fig. 6), probably due to the formation of dimer(s) (Scheme 1) [86–89].

The spectral changes recorded for the solution at pH 3.0 during electrolysis at −1.00 V (Fig. 8B) resemble those previously discussed for the solution at pH 6.5.

In summary, the spectroelectrochemical measurements indicate that the reduction of the pyridinium groups takes place prior to that of the porphyrin core.

4. Summary

Regarding the photophysical properties, $ZnOEP(Py)_4{}^{4+}$ must be classified as a distorted porphyrin. Its UV–vis absorption spectrum displays red-shifted and broader Soret and Q bands with reduced extinction coefficients compared to planar analogues. The

properties of its S_1 state (short lifetime of 170 ps and low fluorescence quantum yield of 0.0025) are comparable with those reported for saddle-shaped porphyrins. Indeed, internal conversion and intersystem crossing to the triplet state T_1 are favoured by the distortions of the macrocycle. The T_1 state also have a shortened lifetime compared to that of $ZnTMPyP^{4+}$.

The electrochemical study of $[ZnOEP(Py)_4{}^{4+},4Cl^-]$ has revealed two different reduction patterns of the pyridinium substituents according to pH. A reduction in four distinct steps takes place at pH 6.5 while a one plus three electrons scheme is observed at pH 3.0. In both cases the pyridinium groups undergo electron transfers before the macrocycle ring. In contrast to the rule that deformed porphyrins are easier to oxidize than planar corresponding porphyrins one, $[ZnOEP(Py)_4{}^{4+},4Cl^-]$ is found harder to oxidize than the planar "analogue" $ZnTMPyP^{4+}$. In addition, the electrochemical processes are irreversible, dimerization after reduction of the generated pyridyl radicals and attack by the solvent of the oxidized porphyrin being the most probable side reactions.

Acknowledgments

This work was supported by CNRS, Université Paris-Sud 11 (Orsay, France) and Université de Strasbourg (Strasbourg, France). The ANR agency is acknowledged for providing financial support, (Project no. JC05_52437, NCPPOM, N.K. post-doctoral grant). The authors would also like to thank M. Erard for the time-resolved fluorescence measurements.

References

[1] S. Fukuzumi, Electron transfer chemistry of porphyrins and metalloporphyrins, in: K.M. Kadish, K.M. Smith, R. Guilard (Eds.), The Porphyrin Handbook, vol. 8, Academic Press, San Diego, 2000, pp. 115–152.
[2] B. Meunier, Metalloporphyrins as versatile catalysts for oxidation reactions and oxidative DNA cleavage, Chem. Rev. 92 (1992) 1411–1456.
[3] M. Tabata, K. Nakajima, E. Nyarko, Metalloporphyrin mediated DNA cleavage by a low concentration of HaeIII restriction enzyme, J. Inorg. Biochem. 78 (2000) 383–389.
[4] R. Bonnet, Photosensitizers of the porphyrin and phthalocyanine series for photodynamic therapy, Chem. Soc. Rev. 24 (1995) 19–33.
[5] R.W. Boyle, D. Dolphin, Structure and biodistribution relationships of photodynamic sensitizers, Photochem. Photobiol. 64 (1996) 469–485.
[6] E.D. Sternberg, D. Dolphin, C. Brückner, Porphyrin-based photosensitizers for use in photodynamic therapy, Tetrahedron 54 (1998) 4151–4202.
[7] D.A. James, N. Swamy, N. Paz, R.N. Hanson, R. Ray, Synthesis and estrogen receptor binding affinity of a porphyrin-estradiol conjugate for targeted photodynamic therapy of cancer, Bioorg. Med. Chem. Lett. 9 (1999) 2379–2384.
[8] R.K. Pandey, G. Zheng, Porphyrins as photosensitizers in photodynamic therapy, in: K.M. Kadish, K.M. Smith, R. Guilard (Eds.), The Porphyrin Handbook, vol. 6, Academic Press, San Diego, 2000, pp. 157–230.
[9] H.L. Kee, J. Bhaumik, J.R. Diers, P. Mroz, M.R. Hamblin, D.F. Bocian, J.S. Lindsey, D. Holten, Photophysical chracterization of imidazolium-substituted Pd(II), In(II), and Zn(II) porphyrins as photosensitizers for photodynamic therapy, J. Photochem. Photobiol. A: Chem. 200 (2008) 346–355.
[10] N.V. Anantha, M. Azam, R.D. Sheardy, Porphyrin binding to quadruplexed T_4G_4, Biochemistry 37 (1998) 2709–2714.
[11] R.T. Wheelhouse, D. Sun, H. Han, F.X. Han, L.H. Hurley, Cationic porphyrins as telomerase inhibitors: the interaction of tetra-(N-methyl-4-pyridyl)porphine with quadruplex DNA, J. Am. Chem. Soc. 120 (1998) 3261–3262.
[12] A.B. Guliaev, N.B. Leontis, Cationic 5,10,15,20-tetrakis(N-methylpyridinium-4-yl)porphyrin fully intercalates at 5′-CG-3′ steps of duplex DNA in solution, Biochemistry 38 (1999) 15425–15437.
[13] O.Y. Fedoroff, A. Rangan, V.V. Chemeris, L.H. Hurley, Cationic porphyrins promote the formation of i-Motif DNA and bind peripherally by a nonintercalative mechanism, Biochemistry 39 (2000) 15083–15090.
[14] T. Uno, K. Aoki, T. Shikimi, Y. Hiranuma, Y. Tomisugi, Y. Ishikawa, Copper insertion facilitates water-soluble porphyrin binding to rA·rU and rA·dT base pairs in duplex RNA and RNA·DNA hybrids, Biochemistry 41 (2002) 13059–13066.
[15] K. Zupan, L. Herenyi, K. Toth, Z. Majer, G. Csik, Binding of cationic porphyrin to isolated and encapsidated viral DNA analyzed by comprehensive spectroscopic methods, Biochemistry 43 (2004) 9151–9159.
[16] J. Kang, H. Wu, X. Lu, Y. Wang, L. Zhou, Study on the interaction of new water-soluble porphyrin with DNA, Spectrochim. Acta Part A 61 (2005) 2041–2047.
[17] M. Ravikanth, T.K. Chandrashekar, Nonplanar porphyrins and their biological relevance: ground and excited state dynamics, Struct. Bonding 82 (1995) 105–188.
[18] J.A. Shelnutt, X.Z. Song, J.G. Ma, S.L. Jia, W. Jentzen, C.J. Medforth, Nonplanar porphyrins and their significance in proteins, Chem. Soc. Rev. 27 (1998) 31–41.
[19] J. Fajer, Structural effects in chemistry and biology, J. Porphyrins Phthalocyanines 4 (2000) 382–385.
[20] L.D. Sparks, C.J. Medforth, M.S. Park, J.R. Chamberlain, M.R. Ondrias, M.O. Senge, K.M. Smith, J.A. Shelnutt, Metal dependence of the nonplanar distortion of octaalkyltetraphenylporphyrins, J. Am. Chem. Soc. 115 (1993) 581–592.
[21] F. D'Souza, M.E. Zandler, P. Tagliatesta, Z. Ou, J. Shao, E. Van Caemelbecke, K.M. Kadish, Electronic, spectral, and electrochemical properties of $(TPPBr_x)Zn$ where $TPPBr_x$ is the dianion of β-brominated-pyrrole tetraphenylporphyrin and x varies from 0 to 8, Inorg. Chem. 37 (1998) 4567–4572.
[22] M.O. Senge, Exercises in molecular gymnastics—bending, stretching and twisting porphyrins, Chem. Commun. (2006) 243–256.
[23] I. Batinic-Haberle, I. Spasojevic, P. Hambright, L. Benov, A.L. Crumbliss, I. Fridovich, Relationship among redox potentials, proton dissociation constants of pyrrolic nitrogens, and in vivo and in vitro superoxide dismutating activities of manganese(III) and iron(III) water-soluble porphyrins, Inorg. Chem. 38 (1999) 4011–4022.
[24] A.B.J. Parusel, T. Wondimagegn, A. Ghosh, Do nonplanar porphyrins have red-shifted electronic spectra? A DFT/SCI study and reinvestigation of a recent proposal, J. Am. Chem. Soc. 122 (2000) 6371–6374.
[25] H. Ryeng, A. Ghosh, Do nonplanar distortions of porphyrins bring about strongly red-shifted electronic spectra? Controversy, consensus, new developments, and relevance to chelatases, J. Am. Chem. Soc. 124 (2002) 8099–8103.
[26] R.E. Haddad, S. Gazeau, J. Pécaut, J.-C. Marchon, C.J. Medforth, J.A. Shelnutt, Origin of the red shifts in the optical absorption bands of nonplanar tetraalkylporphyrins, J. Am. Chem. Soc. 125 (2003) 1253–1268.
[27] K.M. Barkigia, L. Chantranupong, K.M. Smith, J. Fajer, Structural and theoretical models of photosynthetic chromophores. Implications for redox, light-absorption properties and vectorial electron flow, J. Am. Chem. Soc. 110 (1988) 7566–7567.
[28] A. Regev, T. Galili, C.J. Medforth, K.M. Smith, K.M. Barkigia, J. Fajer, H. Levanon, Triplet dynamics of conformationally distorted porphyrins: time-resolved electron paramagnetic resonance, J. Phys. Chem. 98 (1994) 2520–2526.
[29] S. Gentemann, C.J. Medforth, T.P. Forsyth, D.J. Nurco, K.M. Smith, J. Fajer, D. Holten, Photophysical properties of conformationally distorted metal-free porphyrins. Investigation into the deactivation mechanisms of the lowest excited singlet state, J. Am. Chem. Soc. 116 (1994) 7363–7368.
[30] S. Gentemann, C.J. Medforth, E. Tadashi, N.Y. Nelson, K.M. Smith, J. Fajer, D. Holtena, Unusual picosecond $^1(\pi, \pi^*)$ deactivation of ruffled nonplanar porphyrins, Chem. Phys. Lett. 245 (1995) 441–447.
[31] N.C. Maiti, M. Ravikanth, Fluorescence study of some deformed zinc(II) porphyrins, J. Photochem. Photobiol. A: Chem. 101 (1996) 7–10.
[32] M.O. Senge, M.W. Renner, W.W. Kalisch, J. Fajer, Molecular structure of (5,10,15,20-tetrabutyl-2,3,7,8,12,13,17,18-octaethylporphyrinato)nickel(II)—correlation of nonplanarity with frontier orbital shifts, J. Chem. Soc., Dalton Trans. (2000) 381–385.
[33] T. Nakanishi, K. Ohkubo, T. Kojima, S. Fukuzumi, Reorganisation energies of diprotonated and saddle-distorted porphyrins in photoinduced electron-transfer reduction controlled by conformational distortion, J. Am. Chem. Soc. 131 (2009) 577–584.
[34] A. Giraudeau, S. Lobstein, L. Ruhlmann, D. Melamed, K.M. Barkigia, J. Fajer, Electrosynthesis, electrochemistry, and crystal structure of the tetracationic Zn-*meso*-tetrapyridiniumyl-β-octaethylporphyrin, J. Porphyrins Phthalocyanines 5 (2001) 793–797.
[35] D. Schaming, A. Giraudeau, S. Lobstein, R. Farha, M. Goldmann, J.P. Gisselbrecht, L. Ruhlmann, Electrochemical behavior of the tetracationic porphyrins $(py)ZnOEP(py)_4{}^{4+}$ $4PF_6{}^-$ and $ZnOEP(py)_4{}^{4+}$ $4Cl^-$, J. Electroanal. Chem. 635 (2009) 20–28.
[36] C. Bernard, J.P. Gisselbrecht, M. Gross, E. Vogel, M. Lausmann, Redox properties of porphycenes and metalloporphycenes. A comparison with porphyrins, Inorg. Chem. 33 (1994) 2393–2401.
[37] X. Liu, K.L. Yeow, S. Velate, R.P. Steer, Photophysics and spectroscopy of the higher electronic states of zinc metalloporphyrins: a theoretical and experimental study, Phys. Chem. Chem. Phys. 8 (2006) 1298–1309.
[38] K. Kalyanasundaram, Photochemistry of water-soluble porphyrins: comparative study of isomeric tetrapyridyl- and tetrakis(*N*-methylpyridiniumyl)porphyrins, Inorg. Chem. 23 (1984) 2453–2459.
[39] K.M. Barkigia, M.D. Berber, J. Fajer, C.J. Medforth, M.W. Renner, K.M. Smith, Nonplanar porphyrins. X-ray structures of (2,3,7,8,12,13,17,18-octaethyl- and -octamethyl-5,10,15,20-tetraphenylporphinato)zinc(II), J. Am. Chem. Soc. 112 (1990) 8851–8857.
[40] J. Rochford, S. Botchway, J.J. McGarvey, A.D. Rooney, M.T. Pryce, Photophysical and electrochemical properties of *meso*-substituted thien-2-yl Zn(II) porphyrins, J. Phys. Chem. A 112 (2008) 11611–11618.
[41] K. Kalyanasundaram, M. Neumann-Spallart, Photophysical and redox properties of water-soluble porphyrins in aqueous media, J. Phys. Chem. 86 (1982) 5163–5169.
[42] W. Jentzen, M.C. Simpson, J.D. Hobbs, X. Song, T. Ema, N.Y. Nelson, C.J. Medforth, K.M. Smith, M. Veyrat, et al., Ruffling in a series of nickel(II) meso-tetrasubstituted porphyrins as a model for the conserved ruffling of the heme of cytochromes c, J. Am. Chem. Soc. 117 (1995) 11085–11097.
[43] S. Gentemann, N.Y. Nelson, L. Jaquinod, D.J. Nurco, S.H. Leung, C.J. Medforth, K.M. Smith, J. Fajer, D. Holten, Variations and temperature dependence of the excited state properties of conformationally and electronically perturbed zinc and free base porphyrins, J. Phys. Chem. B 101 (1997) 1247–1254.

[44] I.V. Sazanovitch, V.A. Galievski, A. van Hoek, T.J. Schaaffsma, V.L. Malinovskii, D. Holten, V.S. Chirvony, Photophysical and structural properties of saddle-shaped free base porphyrins: evidence for an "orthogonal" dipole moment, J. Phys. Chem. B 105 (2001) 7818–7829.
[45] T. Ema, M.O. Senge, N.Y. Nelson, H. Ogoshi, K.M. Smith, 5,10,15,20-Tetra-tert-butylporphyrin and its remarkable reactivity in the 5- and 15-positions, Angew. Chem. Int. Ed. Engl. 33 (1994) 1879–1881.
[46] J. Karolczak, D. Kowalska, A. Lukaszewicz, A. Maciejewski, R.P. Steer, Photophysical studies of porphyrins and metalloporphyrins: accurate measurements of fluorescence spectra and fluorescence quantum yields for Soret band excitation of zinc tetraphenylporphyrin, J. Phys. Chem. A 108 (2004) 4570–4575.
[47] A. Harriman, G. Porter, M.C. Richoux, Photosensitised reduction of water to hydrogen using water-soluble zinc porphyrins, J. Chem. Soc., Faraday Trans. 2 (77) (1981) 833–844.
[48] V.H. Houlding, K. Kalyanasundaram, M. Grätzel, Kinetics of triplet decay of water soluble porphyrins. Analysis of ionic strength effects, J. Phys. Chem. 87 (1983) 3175–3179.
[49] S. Akimotoa, T. Yamazakia, I. Yamazakia, A. Osukab, Excitation relaxation of zinc and free-base porphyrin probed by femtosecond fluorescence spectroscopy, Chem. Phys. Lett. 309 (1999) 177–182.
[50] M. Enescu, K. Steenkeste, F. Tfibel, M.-P. Fontaine-Aupart, Femtosecond relaxation processes from upper excited states of tetrakis(N-methyl-4-pyridyl)porphyrins studied by transient absorption spectroscopy, Phys. Chem. Chem. Phys. 4 (2002) 6092–6099.
[51] G.G. Gurzadyan, T.-H. Tran-Thi, T. Gustavsson, Time-resolved fluorescence spectroscopy of high-lying electronic states of Zn-tetraphenylporphyrin, J. Chem. Phys. 108 (1998) 385–388.
[52] M. Andersson, J. Davidsson, L. Hammarstrom, J. Korppi-Tommola, T. Peltola, Photoinduced electron transfer reactions in a porphyrin-viologen complex: observation of S_2 to S_1 relaxation and electron transfer from the S_2 State, J. Phys. Chem. B 103 (1999) 3258–3262.
[53] H.Z. Yu, J.S. Baskin, A.H. Zewail, Ultrafast dynamics of porphyrins in the condensed phase: II. Zinc tetraphenylporphyrin, J. Phys. Chem. A 106 (2002) 9845–9854.
[54] H. Chosrowjan, S. Tanigichi, T. Okada, S. Takagi, T. Arai, K. Tokumam, Electron transfer quenching of S_2 state fluorescence of Zn-tetraphenylporphyrin, Chem. Phys. Lett. 242 (1995) 644–649.
[55] M. Vacha, S. Machida, K. Horie, Relaxations of the second excited state of zinc tetraphenylporphyrin probed by spectral hole burning in the Soret absorption band: electron transfer versus internal conversion, J. Phys. Chem. 99 (1995) 13163–13167.
[56] R.H. Felton, in: D. Dolphin (Ed.), The Porphyrins, Academic Press, New York, 1978, p. 53.
[57] K.M. Kadish, E. Van Caemelbecke, G. Royal, in: K.M. Kadish, K.M. Smith, R. Guilard (Eds.), The Porphyrin Handbook, vol. 8, Academic Press, New York, 2000, p. 1.
[58] L. El Kahef, M. Gross, A. Giraudeau, β-substitutions on *meso*-tetraphenylporphyrin by direct electrochemical oxidation in the presence of nucleophiles, J. Chem. Soc. Chem. Commun. (1989) 963.
[59] L. Ruhlmann, A. Giraudeau, One-pot electrochemical generation of a porphyrin dimer with bis(diphenylphosphonium)acetylene bridge, J. Chem. Soc., Chem. Commun. (1996) 2007–2008.
[60] L. Ruhlmann, S. Lobstein, M. Gross, A. Giraudeau, An electrosynthetic path toward pentaporphyrins, J. Org. Chem. 64 (1999) 1352–1355.
[61] L. Ruhlmann, A. Schulz, A. Giraudeau, C. Messerschmidt, J.H. Fuhrhop, A polycationic zinc-5,15-dichlorooctaethylporphyrinate-viologen wire, J. Am. Chem. Soc. 121 (1999) 6664–6667.
[62] L. Ruhlmann, A. Giraudeau, A first series of dimeric porphyrins electrochemically linked with diphosphonium bridges, Eur. J. Inorg. Chem. (2001) 659–668.
[63] L. Ruhlmann, M. Gross, A. Giraudeau, Bisporphyrins with bischlorin features obtained by direct anodic coupling of porphyrins, Chem. Eur. J. 9 (2003) 5085–5096.
[64] J. Hao, A. Giraudeau, Z. Ping, L. Ruhlmann, Supramolecular assemblies obtained by large counteranion incorporation in a well-oriented polycationic copolymer, Langmuir 24 (2008) 1600–1603.
[65] L. Ruhlmann, J. Hao, Z. Ping, A. Giraudeau, Self-oriented polycationic copolymers obtained from bipyridinium *meso*-substituted-octaethylporphyrins, J. Electroanal. Chem. 621 (2008) 22–30.
[66] T. Malinsky, D. Chang, J.M. Latour, J.C. Marchon, M. Gross, A. Giraudeau, K.M. Kadish, Electrochemistry of oxo- and peroxotitanium(IV) porphyrins. Mechanism of the two-electron reduction of a η^2-coordinated peroxo ligand, Inorg. Chem. 23 (1984) 3947–3955.
[67] P. Hambright, Chemistry of water soluble porphyrins, in: K.M. Kadish, K.M. Smith, R. Guilard (Eds.), The Porphyrin Handbook, vol. 3, Academic Press, San Diego, 2000, pp. 129–200.
[68] A. Bettelheim, T. Kuwana, Rotating-ring-disk analysis of iron tetra(N-methylpyridyl)porphyrin in electrocatalysis of oxygen, Anal. Chem. 51 (1979) 2257–2260.
[69] M. Neumann-Spallart, K. Kalyanasundaram, On the one and two-electron oxidations of water soluble zinc porphyrins in aqueous media, Z. Naturforsch. B 36 (1981) 596–600.
[70] A. Harriman, M.C. Richoux, P. Neta, Redox chemistry of metalloporphyrins in aqueous solution, J. Phys. Chem. 87 (1983) 4957–4985.
[71] S. Baral, P. Hambright, P. Neta, One- and two-electron reduction of aluminum and tin pyridylporphyrins. A kinetic spectrophotometric study, J. Phys. Chem. 88 (1984) 1595–1600.
[72] K.W. Morehouse, P. Neta, Redox reactions of manganese porphyrins in aqueous solutions. Steady-state and pulse radiolysis spectrophotometric studies, J. Phys. Chem. 88 (1984) 1575–1579.
[73] M.C. Richoux, P. Neta, A. Harriman, S. Baral, P. Hambright, One- and two-electron reduction of metalloporphyrins. Radiation chemical, photochemical, and electrochemical studies. Kinetics of the decay of π-radical anions, J. Phys. Chem. 90 (1986) 2462–2468.
[74] Z.M. Abou-Gamra, A. Harriman, P. Neta, Redox chemistry of Gold(III) porphyrins in water, J. Chem. Soc., Faraday Trans. 2 (1986) 2337–2350.
[75] P. Hambright, P. Neta, M.C. Richoux, Z.M. Abou-Gamra, A. Harriman, Redox chemistry of water-soluble vanadyl porphyrins, J. Photochem. 36 (1987) 255–265.
[76] Z.M. Abou-Gamra, N.M. Guindy, Photochemistry of metalloporphyrins in aqueous solutions, Spectrochim. Acta 45A (1989) 1207–1210.
[77] C. Zhou, Y. Ni, X. Gao, Voltammetric study of zinc-tetrakis(N-methyl-4-pyridinium)porphyrin, Chin. Sci. Bull. 36 (1991) 827–830.
[78] K.M. Kadish, D. Sazou, M. Liu, A. Saoiabi, M. Ferhat, R. Guilard, Electrochemical and spectral characterization of the monomer-dimer equilibrium involving (*meso*-tetrakis(1-methylpyridinium-4-yl)porphinato)nickel(II) in dimethylformamide, Inorg. Chem. 27 (1988) 686–690.
[79] K.M. Kadish, C. Araullo, G.B. Maiya, D. Sazou, J.M. Barbe, R. Guilard, Electrochemical and spectral characterization of copper, zinc, and vanadyl *meso*-tetrakis(1-methylpyridinium-4-yl)porphyrin complexes in dimethylformamide, Inorg. Chem. 28 (1989) 2528–2533.
[80] C. Araullo, K.M. Kadish, Electrochemistry, spectroscopy, and reactivity of (*meso*-tetrakis(1-methylpyridinium-4-yl)porphinato)cobalt(III,II,I) in non-aqueous media, Inorg. Chem. 29 (1990) 2749–2757.
[81] E. Van Caemelbecke, W. Kutner, K.M. Kadish, Electrochemical and spectroelectrochemical characterization of (5,10,15,20-tetrakis(1-methyl-4-pyridyl)porphinato)manganese(III) chloride, $[(TMpyP)MnIIICl]^{4+}(Cl^-)_4$, in N,N-dimethylformamide, Inorg. Chem. 32 (1993) 438–444.
[82] E. Van Caemelbecke, A. Derbin, P. Hambright, R. Garcia, A. Doukkali, A. Saoiabi, K. Ohkubo, S. Fukuzumi, K.M. Kadish, Electrochemistry of $[(TMpyP)M^{II}]^{4+}(X^-)_4$ ($X^- = Cl^-$ or BPh_4^-) and $[(TMpyP)M^{III}Cl]^{4+}$ $(Cl^-)_4$ in N,N-dimethylformamide where M is one of 15 different metal ions, Inorg. Chem. 44 (2005) 3789–3798.
[83] D. Dolphin, Spectro-electrochemistry: porphyrins and metalloporphyrins, in: T.G. Truscott, R.V. Bensasson, G. Jori, E.J. Land (Eds.), Primary Photo-Processes in Biology and Medicine NATO ASI Series, Series A: Life Sciences, vol. 85, Plenum Publishing Corporation, 1985, pp. 171–180.
[84] B.P. Neri, G.S. Wilson, Electrochemical studies of *meso*-tetra(4-N-methylpyridyl)porphine in acid solution, Anal. Chem. 44 (1972) 1002–1009.
[85] I. Prieto, M.T. Martin, D. Möbius, L. Camacho, Electrochemical properties of Langmuir–Blodgett mixed films consisting of a water-soluble porphyrin and a phospholipid, J. Phys. Chem. B 102 (1998) 2523–2529.
[86] M.A. Oturan, P. Dostert, M. Strolin-Benedetti, J. Moiroux, A. Anne, M.B. Fleury, One-electron and two-electron reductions of 1-methyl-4-phenyl-pyridinium (MPP^+), J. Electroanal. Chem. 242 (1988) 171.
[87] V. Carelli, F. Liberatore, A. Casini, S. Tortorella, L. Scipione, B. Di Rienzo, On the regio- and stereoselectivity of pyridinyl radical dimerization, New J. Chem. (1998) 999–1004.
[88] J.E.H. Buston, F. Marken, H.L. Anderson, Enhanced chemical reversibility of redox processes in cyanine dye rotaxanes, Chem. Comm. (2001) 1046–1047.
[89] V. Carelli, F. Liberatore, S. Tortorella, B. Di Rienzo, L. Scipione, Structure of the dimers arising from one-electron electrochemical reduction of pyridinium salts 3,5-disubstituted with electron-withdrawing groups, J. Chem. Soc., Perkin Trans. 1 (2002) 542–547.